ACS APPLIED MATERIALS & INTERFACES

Research Article

www.acsami.org

Ultrafast Oleophobic–Hydrophilic Switching Surfaces for Antifogging, Self-Cleaning, and Oil–Water Separation

P. S. Brown, O. D. L. A. Atkinson, and J. P. S. Badyal*

Department of Chemistry Science Laboratories, Durham University, Durham DH1 3LE, United Kingdom

ABSTRACT: Smooth copolymer–fluorosurfactant complex film surfaces are found to exhibit fast oleophobic–hydrophilic switching behavior. Equilibration of the high oil contact angle (hexadecane = 80°) and low water contact angle (<10°) values occurs within 10 s of droplet impact. These optically transparent surfaces display excellent antifogging and self-cleaning properties. The magnitude of oleophobic–hydrophilic switching can be further enhanced by the incorporation of surface roughness to an extent that it reaches a sufficiently high level (water contact angle <10° and hexadecane contact angle >110°), which, when combined with the inherent ultrafast switching speed, yields oil–water mixture separation efficiencies exceeding 98%.

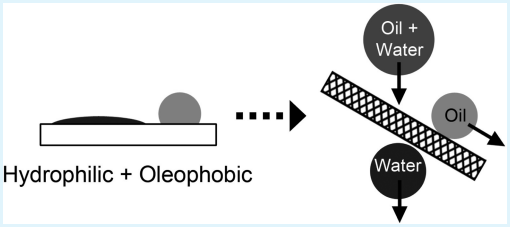

KEYWORDS: *oleophobic–hydrophilic, switching surface, antifogging, self-cleaning, oil–water separation, copolymer–fluorosurfactant complex*

1. INTRODUCTION

Because ot the frequency of off-shore oil spillages[1,2] and the emergence of fracking (where water-based fluids are used to fracture rocks for the release of oil and gas), the separation of oil and water is an important environmental challenge.[3−8] Existing methods for the removal or collection of oils from an oil–water mixture utilize absorbent materials[9] such as zeolites,[10,11] organoclays,[12] nonwoven polypropylene,[13,14] or natural fibers[15] (such as straw,[16] cellulose,[14] or wool[17]). However, these materials also tend to absorb water, thereby lowering their efficiency.[18] In addition, extra steps are necessary in order to remove the absorbed oil from the material, which makes such methods highly incompatible with continuous-flow systems (e.g., attached to cleanup marine vessels). There also exist separation membranes that repel one liquid phase while allowing the other to pass through. Typically these are made out of hydrophobic and oleophilic materials,[19−21] causing water to run off the surface while allowing oil to permeate through. Their main drawback tends to be surface contamination with oil, culminating in a drop in the separation efficiency.[22,23] The most attractive approach to date appears to be the utilization of oleophobic–hydrophilic surfaces where the oil and oil-based contaminants are repelled and water passes through.[24] Such surfaces are also of interest for self-cleaning,[25−27] antifogging,[25,28,29] and antifouling[30,31] applications.

One important class of oleophobic–hydrophilic surfaces is polyelectrolyte–surfactant complexes,[32,33] where the surfactant is attached to the polyelectrolyte via an oppositely charged electrostatic interaction.[34,35] In the case of polyelectrolyte–fluorosurfactant complexes, the fluorinated alkyl chains can orient toward the air–solid interface to provide a low-surface-energy film. Such alignment localizes hydrophilic portions of the polyelectrolyte in the near-surface region by electrostatic attraction.[36] This means that when water is placed onto the surface, it penetrates through defects in the fluorinated outermost layer toward the hydrophilic subsurface, giving rise to a "switch" of the surface–water interaction from hydrophobic to hydrophilic.[37] Larger oil molecules are unable to penetrate through this top layer, leaving the surface oleophobic.[37] Earlier polyelectrolyte–surfactant complex oleophobic–hydrophilic surfaces have been impeded from more widespread usage because of several factors: it can take several minutes for the water to penetrate through the fluorinated top layer, resulting in a surface that is initially hydrophobic,[38,39] and the level of oil repellency is quite poor (hexadecane contact angles of only 70° or lower[40−42]). Pulsed-plasma-deposited poly(maleic anhydride) and poly(acrylic acid) surfaces that are subsequently complexed to fluorosurfactant display better oleophobicity;[32,33] however, the two-step process is unsuitable for many large-scale industrial applications.

In this study, fast-switching oleophobic–hydrophilic polyelectrolyte–fluorosurfactant surfaces have been prepared in a single step, utilizing three different maleic anhydride copolymers (so as to systematically investigate the role of the polymer backbone structure; Scheme 1). These comprised a poly(ethylene-*alt*-maleic anhydride) alternating copolymer as a reference standard (based on previously reported polyelectrolyte–fluorosurfactant switching studies[32]), poly(styrene-*alt*-maleic anhydride) where the aforementioned alternating copolymer ethylene segments are replaced with styrene segments, and finally poly(styrene-*co*-maleic anhydride), which is a copolymer consisting of single maleic anhydride units alternating with styrene block segments (because maleic anhydride does not homopolymerize[43]).

Received: February 11, 2014
Accepted: April 14, 2014
Published: April 30, 2014

dx.doi.org/10.1021/am500882y | *ACS Appl. Mater. Interfaces* 2014, 6, 7504−7511

Scheme 1. Maleic Anhydride Copolymers and Cationic Fluorosurfactant Used To Prepare Copolymer–Fluorosurfactant Complexes

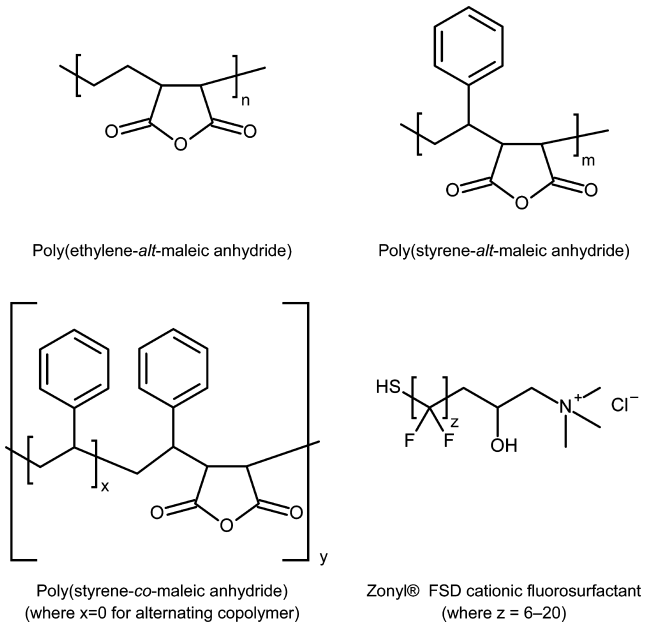

2. EXPERIMENTAL SECTION

Polished silicon (100) wafers (Silicon Valley Microelectronics, Inc.) and glass slides (Academy Science Ltd.) were used as flat substrates. Poly(ethylene-*alt*-maleic anhydride) [poly(Et-*alt*-MA); Vertellus Specialties Inc.], poly(styrene-*alt*-maleic anhydride) [poly(St-*alt*-MA); Apollo Scientific Ltd.], or poly(styrene-*co*-maleic anhydride) [poly(St-*co*-MA); Polyscope Polymers BV] were dissolved in acetone (+99.8%, Sigma-Aldrich Ltd.) at a concentration of 2% (w/v). The aqueous cationic fluorosurfactant (Zonyl FSD; DuPont Ltd.) employed for complexation was further diluted in high-purity water at a concentration of 5% (v/v) and then added to the copolymer solution, resulting in hydrolysis of the maleic anhydride ring contained in the polymer and leading to the formation of a polyelectrolyte–surfactant complex. The precipitated solid was collected from the liquid phase and dissolved at a concentration of 2% (w/v) in dimethylformamide (DMF, 99%; Fisher Scientific UK Ltd.) for the preparation of smooth surfaces, and in the case of the poly(St-*co*-MA)–fluorosurfactant complex, varying composition DMF–methanol (99%, Sigma-Aldrich Ltd.) solvent mixtures were utilized to produce rough surfaces. Spin coating was carried out using a photoresist spinner (Cammax Precima) operating at 2000 rpm. For the oil–water separation experiments, stainless steel mesh (0.16 mm wire diameter, 0.20 mm square holes, The Mesh Company Ltd.) was dip-coated in the copolymer–fluorosurfactant complex solution and the solvent allowed to evaporate.

Glass transition temperatures of the copolymer and copolymer–fluorosurfactant complexes were measured by differential scanning calorimetry (DSC; Pyris 1, PerkinElmer Inc.).

Microliter sessile drop contact angle analysis was carried out with a video capture system (VCA2500XE, AST Products Inc.) using 1.0 μL dispensation of deionized water (BS 3978 grade 1), hexadecane (99%, Sigma-Aldrich Ltd.), tetradecane (+99%, Sigma-Aldrich Ltd.), dodecane (99%, Sigma-Aldrich Ltd.), decane (+99%, Sigma-Aldrich Ltd.), octane (+99%, Sigma-Aldrich Ltd.), heptane (99%, Sigma-Aldrich Ltd.), hexane (+99%, Sigma-Aldrich Ltd.), and pentane (+99%, Sigma-Aldrich Ltd.). Advancing and receding contact angles were measured by respectively increasing and decreasing the droplet size until the contact line was observed to move.[44] Oil repellency was further tested using motor engine oil (GTX 15W-40, Castrol Ltd.) and olive cooking oil (Tesco PLC). Switching parameters were determined by calculating the difference between equilibrium hexadecane and water contact angles.

Atomic force microscopy (AFM) images were collected in tapping mode at 20 °C in ambient air (Nanoscope III, Digital Instruments, Santa Barbara, CA) using a tapping mode tip with a spring constant of 42–83 N/m (Nanoprobe). Root-mean-square (rms) roughness values were calculated over 100 × 100 μm scan areas consisting of 256 × 256 lines.

Antifogging was tested by exposing the coated surfaces to a high-purity water spray from a pressurized nozzle (RG-3L, Anest Iwata Inc.).[45] Self-cleaning was tested by dispensing oil droplets onto a surface followed by rinsing with high-purity water. Oil–water separation efficiencies were measured by pouring a vigorously agitated mixture of oil and water over stainless steel mesh that has been dip-coated with a copolymer–fluorosurfactant complex. The steel mesh was inclined at a shallow angle to allow the oil to roll off the mesh surface while the water passed straight through, and the collected amounts were measured. Oil Red O (≥75% dye content, Sigma-Aldrich Ltd.) and Procion Blue MX-R (35% dye content, Sigma-Aldrich Ltd.) were employed as oil- and water-dispersible dyes, respectively, in order to enhance visual contrast (similar results were obtained in the absence of dye). Oil–water separation efficiency was calculated from the volumes of liquid collected using the inclined coated meshes.

3. RESULTS

3.1. Surface Switching. DSC showed that the poly(Et-*alt*-MA) copolymer has a higher glass transition temperature compared to poly(St-*alt*-MA), which can be attributed to the larger molecular weight of the former and less ordering due to the stiff and bulky styrene groups[46] for the latter (Table 1). In the case of the poly(St-*co*-MA) copolymer, the presence of a single glass transition temperature is consistent with block styrene segments alternating with single maleic anhydride units (since a plausible alternative diblock copolymer structure should display two respective glass transition temperatures;[47] Scheme 1). Also, its higher glass transition temperature compared to the poly(St-*alt*-MA) alternating copolymer stems from a combination of higher molecular weight and favorable intermolecular interactions between adjacent styrene units contained within the block styrene segments.[48]

Table 1. Glass Transition Temperatures of Copolymers and Copolymer–Fluorosurfactant Complexes

			glass transition temperature (°C)	
copolymer	maleic anhydride unit content (%)	molecular weight (g/mol)	copolymer	copolymer–fluorosurfactant complex
poly(Et-*alt*-MA)	50	60000	155	157
poly(St-*alt*-MA)	50	50000	120	131
poly(St-*co*-MA)	26	80000	160	138

Following fluorosurfactant complexation, both the poly(Et-*alt*-MA) and poly(St-*alt*-MA) copolymer–fluorosurfactant complexes display raised glass transition temperatures, which suggests a greater degree of ordering upon surfactant complexation and is consistent with previous studies relating to copolymer–surfactant complex systems (Table 1).[49,50] In contrast, the glass transition temperature is lower for the poly(St-*co*-MA)–fluorosurfactant complex compared to that of the parent copolymer (and now fairly close to that of the alternating copolymer–fluorosurfactant complex); this may be

Table 2. Microliter Water and Hexadecane Static Contact Angles for Copolymer Spin-Coated from Acetone Solvent, Copolymer−Fluorosurfactant Complex Surfaces (Smooth) Spin-Coated from DMF Solvent, and Poly(St-*co*-MA)−Fluorosurfactant Complex Surfaces (Rough) Spin-Coated from 33 vol % DMF−66 vol % Methanol[a]

		static water contact angle (deg)		hexadecane contact angle (deg)			
	AFM rms roughness (nm)	0 s	10 s	static	advancing	receding	hysteresis
poly(Et-*alt*-MA)	4.4 ± 1	38 ± 2	22 ± 2	wets			
poly(Et-*alt*-MA)−fluorosurfactant	1.1 ± 0.3	88 ± 2	<10	74 ± 1	76 ± 2	72 ± 2	4 ± 2
poly(St-*alt*-MA)	6.7 ± 1	68 ± 2	66 ± 2	wets			
poly(St-*alt*-MA)−fluorosurfactant	2.7 ± 0.3	<10	<10	80 ± 2	85 ± 2	66 ± 2	19 ± 2
poly(St-*co*-MA)	10.3 ± 1	90 ± 2	90 ± 2	wets			
poly(St-*co*-MA)−fluorosurfactant	5.3 ± 1	36 ± 2	23 ± 2	80 ± 2	88 ± 2	66 ± 2	22 ± 2
poly(St-*co*-MA)−fluorosurfactant 33 vol % DMF−66 vol % methanol	246 ± 3	<10	<10	112 ± 5	125 ± 5	<10	>115

[a]Water droplets were allowed to relax for 10 s to reach equilibrium prior to final static contact angle measurement. No relaxation in the contact angle was observed for hexadecane droplets. AFM surface roughness values are included for comparison.

due to disruption of the favorable intermolecular interactions between adjacent styrene units contained within the block segments (something that is absent for the parent alternating copolymers).[48,51]

Spin coating of all three copolymer−fluorosurfactant complexes dissolved in DMF onto silicon wafers and glass slides produced smooth films (AFM rms roughness = 1−5 nm; Table 2). In all cases, a time period of 10 s was sufficient for the water contact angles to reach their final static values, while hexadecane droplets remained stationary (Figure 1 and Table 2). In fact, both styrene-containing copolymer−fluorosurfactant complex surfaces reach a final static water contact angle value much faster than their ethylene-containing copolymer counterpart, with the poly(St-*alt*-MA)−fluorosurfactant system undergoing instantaneous water wetting. Copolymer−fluorosurfactant complex surfaces prepared using an alternative quaternary ammonium cationic fluorosurfactant (S-106A, Chemguard) displayed similar oleophobic−hydrophilic switching behavior. This was also found to be the case for copolymer−fluorosurfactant complex surfaces created using a cationic copolymer [poly(styrene-*alt*-maleimide), SMA 1000I, Cray Valley HSC] and an anionic fluorosurfactant (Capstone FS-63, Dupont Ltd.). Repeat rinsing of samples in deionized water retained the observed oleophobic−hydrophilic behavior. Control experiments utilizing any of the parent copolymers (in the absence of fluorosurfactant complexation) showed the converse wetting behavior, with an absence of superhydrophilicity and instantaneous spreading of hexadecane droplets (Table 2).

Oil repellency of the poly(Et-*alt*-MA)−fluorosurfactant complex surfaces was found to improve (higher contact angle and lower hysteresis) with increasing hydrocarbon length of straight-chain alkane droplets (Figure 2). A similar trend was

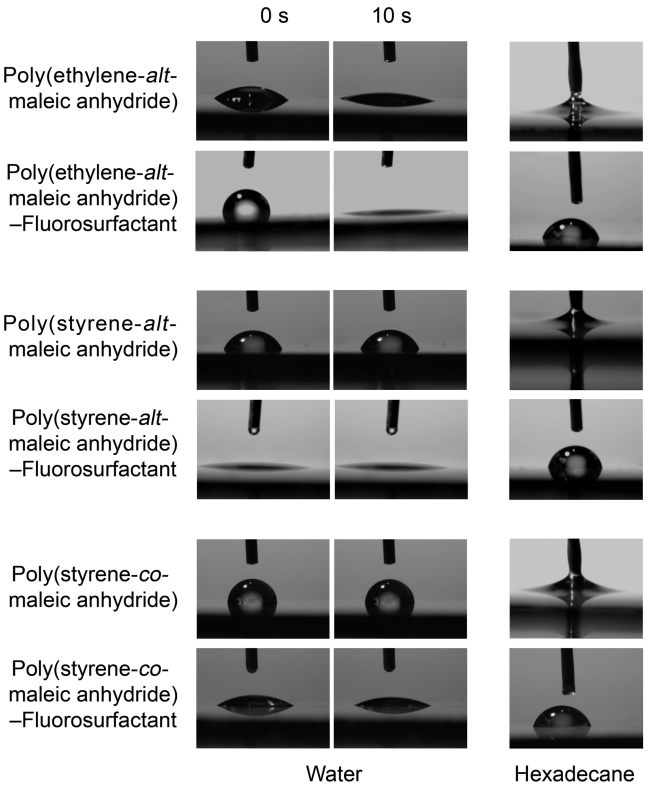

Figure 1. Microliter water and hexadecane droplets dispensed onto copolymer spin-coated from an acetone solvent and copolymer−fluorosurfactant complex surfaces spin-coated from a DMF solvent. No relaxation in the contact angle value was observed for hexadecane droplets.

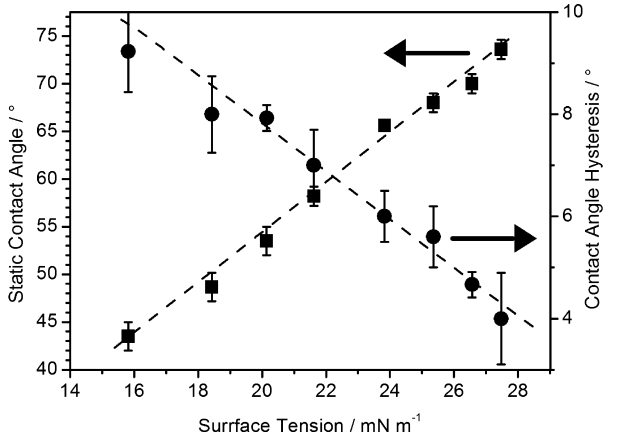

Figure 2. Microliter droplet oil static contact angles and contact angle hysteresis on poly(Et-*alt*-MA)−fluorosurfactant complex surfaces spin-coated from a DMF solvent as a function of liquid straight-chain alkane surface tension. A similar trend was noted for poly(St-*alt*-MA)−fluorosurfactant and poly(St-*co*-MA)−fluorosurfactant surfaces spin-coated from a DMF solvent.

observed for both of the poly(styrene–maleic anhydride)–fluorosurfactant complex surfaces. Furthermore, olive oil and motor engine oil spreading were shown to be inhibited on all three types of copolymer–fluorosurfactant complex surfaces (Figure 3).

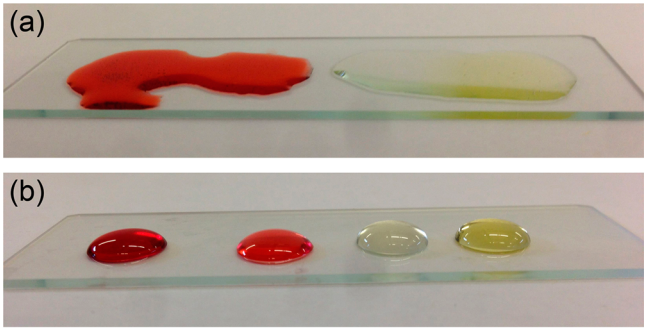

Figure 3. Hexadecane, octane, olive oil, and motor oil droplets (left to right) on (a) an uncoated glass slide and (b) a poly(Et-*alt*-MA)–fluorosurfactant complex surface solvent cast from DMF. A similar trend was noted for poly(St-*alt*-MA)–fluorosurfactant and poly(St-*co*-MA)–fluorosurfactant surfaces spin-coated from a DMF solvent. Hexadecane and octane droplets are dyed with Oil Red O (Sigma-Aldrich Ltd.) to show contrast (similar results were obtained in the absence of dye).

3.2. Antifogging and Self-Cleaning. Extremely low water contact angles are highly desirable for antifogging applications.[52] Copolymer–fluorosurfactant complex dip-coated glass slides using a DMF solvent were found to retain their transparency (antifogging) during liquid water spray exposure (Figure 4).

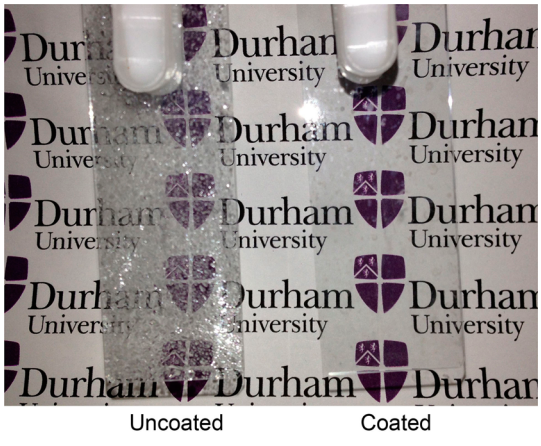

Figure 4. Demonstration of antifogging following exposure to water vapor (fogging): on an uncoated glass slide and a poly(Et-*alt*-MA)–fluorosurfactant complex solvent cast from DMF. Similar behavior was observed for poly(St-*alt*-MA)–fluorosurfactant and poly(St-*co*-MA)–fluorosurfactant complex dip-coated glass slides using a DMF solvent.

Self-cleaning properties for the copolymer–fluorosurfactant dip-coated glass slides were demonstrated by rinsing off fouling oils with just water (Figure 5). This is consistent with the high receding contact angle measured for hexadecane (Table 2).[53]

3.3. Solvent-Induced Roughening To Enhance the Switching Parameter. Further enhancement of the oleophobic–hydrophilic surface switching behavior was investigated for the poly(St-*co*-MA)–fluorosurfactant system by varying the

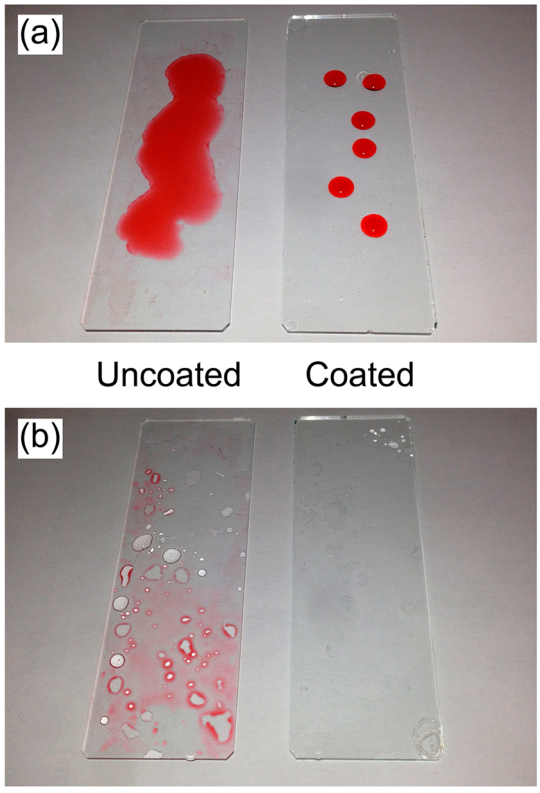

Figure 5. Demonstration of self-cleaning: (a) an uncoated glass slide and a poly(Et-*alt*-MA)–fluorosurfactant complex coating solvent cast from DMF fouled with hexadecane; (b) after a quick rinse with water. Similar behavior was observed for poly(St-*alt*-MA)–fluorosurfactant and poly(St-*co*-MA)–fluorosurfactant complex surface solvents cast from DMF. Hexadecane droplets are dyed with Oil Red O (Sigma-Aldrich Ltd.) to show contrast (similar results were obtained in the absence of dye).

casting solvent mixture composition (Figure 6). Diluting DMF with methanol gives rise to an increase in the surface roughness, which is attributable to the poor solubility of the styrene block segments in methanol.[54] This solvent-induced roughness lowers the static water contact angle (<10°) while concurrently raising the static hexadecane contact angle (>110°), to yield a hexadecane–water switching parameter exceeding 100° (Figure 6b,c). Control experiments showed a lack of surface roughness enhancement by varying the DMF–methanol solvent composition for poly(Et-*alt*-MA)–fluorosurfactant and poly(St-*alt*-MA)–fluorosurfactant complex solutions, which is consistent with the absence of low-methanol-solubility styrene block segments being present in the alternating copolymer structures (Scheme 1).

3.4. Oil–Water Separation. Oil–water separation efficacy was tested using copolymer–fluorosurfactant complex coatings dip-coated onto stainless steel mesh. These were then suspended over a sample vial followed by dispensing an agitated oil–water mixture. The water component was observed to pass through the mesh, while the oil (hexadecane) remained suspended on the mesh surface (Figure 7). These meshes were then inclined at an angle, and pouring the agitated oil–water mixture over them yielded separation efficiencies as high as 98% in the case of the poly(St-*co*-MA)–fluorosurfactant complex surface (attributable to the DMF–methanol solvent-mixture-induced roughness enhancement of the oil–water switching parameter; Figure 7 and Table 3). Inclination of the

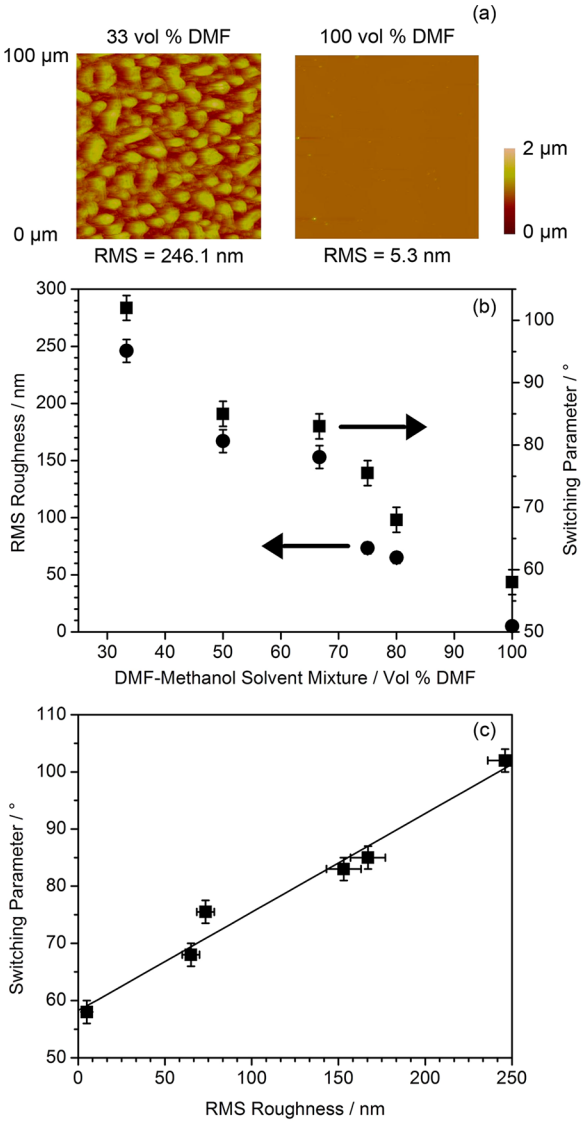

Figure 6. (a) AFM height images and rms roughness values for poly(St-*co*-MA)−fluorosurfactant complex surfaces spin-coated from different vol % DMF−methanol solutions. (b) AFM rms roughness and hexadecane−water static contact angle switching parameter of poly(St-*co*-MA)−fluorosurfactant complex surfaces as a function of the DMF−methanol solvent mixture composition. (c) Correlation between the hexadecane−water static contact angle switching parameter of poly(St-*co*-MA)−fluorosurfactant complex surfaces and the AFM rms roughness.

meshes was required to allow the separated oil to flow downward into an adjacent beaker. The absence of solvent-induced roughness resulted in lower oil−water separation efficiencies for the two alternating copolymer−fluorosurfactant complex systems.

4. DISCUSSION

Polymer−fluorosurfactant complex surfaces, which display oleophobic−hydrophilic switching behavior, rely on the inherent hydrophilicity of the base polymer.[37] For instance, in the case of solvent-cast ionic polymer−fluorosurfactant complex surfaces, the fluorinated surfactant tails segregate at the air−solid interface, thereby aligning the hydrolyzed polymer counterionic groups and ionic surfactant heads toward the near-surface region as a consequence of their strong electrostatic

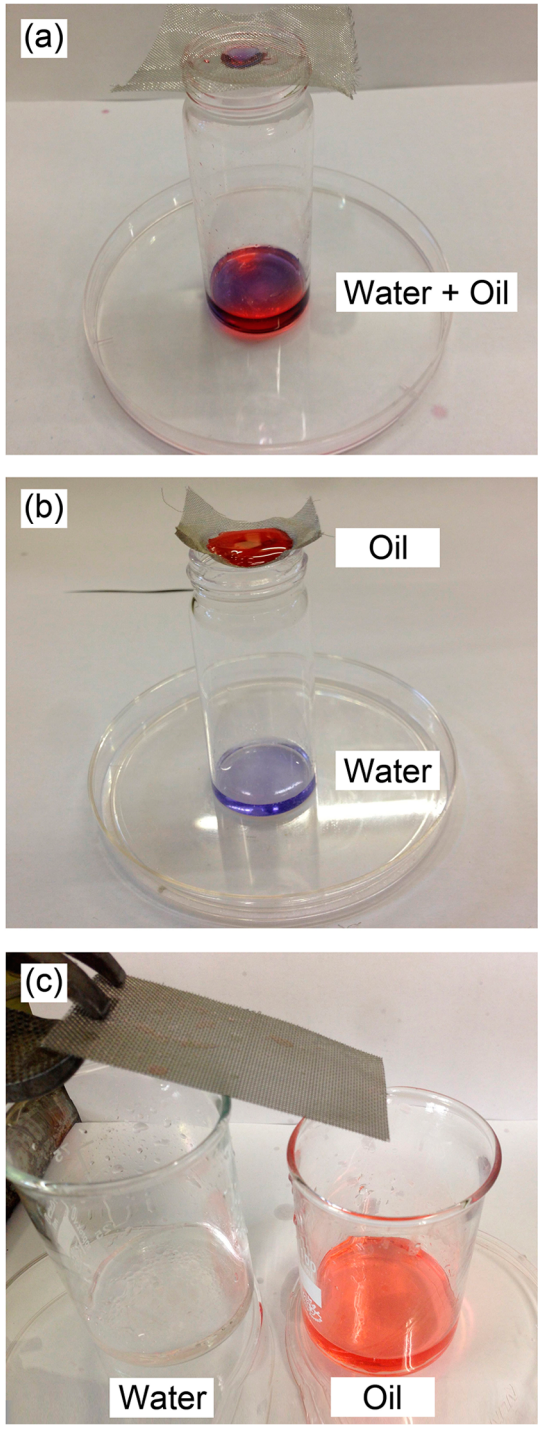

Figure 7. Demonstration of oil−water separation: agitated hexadecane−water mixture dispensed onto (a) uncoated stainless steel mesh, (b) stainless steel mesh dip-coated with the poly(St-*co*-MA)−fluorosurfactant complex in a 33 vol % DMF−66 vol % methanol solvent mixture, and (c) inclined coated stainless steel mesh dip-coated with the poly(St-*co*-MA)−fluorosurfactant complex in a 33 vol % DMF−66 vol % methanol solvent mixture acting as an oil−water separator (oil and water are shown to be collected into separate beakers). Similar behavior was observed for octane−water and motor oil−water mixtures. Hexadecane is dyed with Oil Red O and water with Procion Blue MX-R (in parts a and b) to show contrast (similar results were obtained in the absence of dye).

attraction toward each other.[36,55,56] This interfacial interaction leads to an enhanced concentration of hydrophilic groups in the

Table 3. Oil–Water Separation Efficiencies Using Inclined Meshes for Copolymer–Fluorosurfactant Complex Dip-Coated Stainless Steel Meshes from 33 vol % DMF–66 vol % Methanol Solvent Mixtures

switching surface	AFM rms roughness (nm)	oil–water separation efficiency (%)[a]
poly(Et-*alt*-MA) + fluorosurfactant	1.1 ± 0.3	0
poly(St-*alt*-MA) + fluorosurfactant	2.7 ± 0.3	48 ± 4
poly(St-*co*-MA) + fluorosurfactant	246 ± 3	98 ± 2

[a]100% efficiency corresponds to the complete separation of water from hexadecane.

near-surface region. It has been proposed that such polymer–fluorosurfactant surfaces are able to exhibit oleophobic–hydrophilic switching behavior because of the existence of defect sites or "holes" at the fluorinated surfactant tail air–solid interface through which water molecules can penetrate toward the complexing counterion hydrophilic subsurface.[37] This description helps to explain why all three copolymer–fluorosurfactant complex systems in the present study display lower final static water contact angles compared to their parent base copolymers (Figure 1 and Table 2).

The oleophobic–hydrophilic behavior of such polymer–fluorosurfactant complex surfaces can be quantified in terms of a switching parameter (the difference in the measured static contact angle between hexadecane and water droplets; Figure 8). Furthermore, it can be seen that the copolymer–

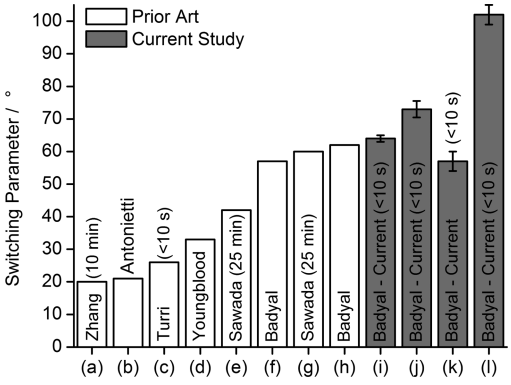

Figure 8. Oleophobic–hydrophilic switching parameters for nominally flat surfaces reported in the literature: (a) Zhang et al.;[39] (b) Antonietti et al.;[40] (c) Turri et al.;[42] (d) Youngblood et al.;[26] (e) Sawada et al.;[38] (f) Badyal et al.;[32] (g) Sawada et al.;[41] (h) Badyal et al.;[33] (i) poly(Et-*alt*-MA)–fluorosurfactant (rms = 1.1 ± 0.3 nm); (j) poly(St-*alt*-MA)–fluorosurfactant (rms = 2.7 ± 0.3 nm); (k) poly(St-*co*-MA)–fluorosurfactant (smooth rms = 5.3 ± 1 nm); (l) poly(St-*co*-MA)–fluorosurfactant (rough rms = 246 ± 3 nm). Switching parameters are calculated from the difference between the hexadecane and water static contact angles. The time it takes for water to reach the final static water contact angle value is given in brackets if reported.

fluorosurfactant complexes employed in the present study significantly outperform earlier reported switching surfaces in terms of this parameter. Most previous studies have tended to quote water contact angles only after allowing the droplet to stabilize over several minutes on the surface because of the slow rate at which water molecules penetrate toward the hydrophilic subsurface in order to manifest surface switching (although the surface initially is hydrophobic).[38,39,41] In the present investigation, the time taken to reach a final static water contact angle is much shorter (<10 s) for all copolymer–fluorosurfactant systems. Furthermore, both styrene-containing copolymer–fluorosurfactant complex surfaces reach a final static water contact angle value quicker than their ethylene-containing copolymer counterpart (and independently from surface roughness) because of the bulky styrene side group providing a lower packing efficiency for the former and thereby facilitating a faster penetration of water into the hydrophilic subsurface (Figure 1). This explanation is consistent with the styrene-based copolymer–fluorosurfactant complexes having lower glass transition temperatures (Table 1). In addition, for the case of the poly(St-*alt*-MA) copolymer, the more disordered nature of the alternating styrene side groups provides a greater level of polymer chain mobility,[57,58] which allows the fluorinated alkyl chains to reorient themselves more readily at the solid–air interface (culminating in instantaneous water wetting and high hexadecane contact angle values; Figure 1 and Table 2).

The high receding hexadecane contact angle and low surface roughness of copolymer–fluorosurfactant complex surfaces spin-coated from a DMF solvent make them ideal for self-cleaning and antifogging applications (Table 2 and Figures 3–5). Such surfaces are easily cleaned by rinsing in water (which replaces the oil–solid interaction with a much more favorable water–solid interaction, i.e., switching).

Dissolving the poly(St-*co*-MA)–fluorosurfactant complex in a DMF–methanol solvent mixture prior to film formation enhances the surface roughness because of the poor solubility of the styrene block segments in methanol.[54] This surface roughness is capable of improving the hydrophilicity due to increased surface area (Wenzel wetting[59]) and the oleophobicity due to the ability to trap air (Cassie–Baxter wetting[60]). See Table 2.[61−63] A key advantage of this approach is that it circumvents the need for introducing roughness as a separate step through the incorporation of additional materials[39,61,64] or by mixing roughening particles into the copolymer–fluorosurfactant complex solution. It is envisaged that a range of different solvents or coating methods (e.g., spray coating[65]) may be used to introduce surface roughness for enhancement of the switching parameter for related polymer–surfactant complex systems.

Coating of the steel mesh with such roughened poly(St-*co*-MA)–fluorosurfactant complex surfaces (prepared from DMF–methanol solvent mixtures) provides hierarchical roughness (two length scales: steel mesh pores plus solvent-induced film roughness) both of which help to lower the oil contact angle hysteresis (improve the oil repellency).[66,67] When combined with the inherent high switching parameter, oil–water separation exceeding >98% efficiency is attained (Table 3). This performance matches the existing oleophobic–hydrophilic systems for oil–water separation (which, however, tend to be far more complex in nature and fabrication methods).[3] Although there are more efficient separation processes (99.999% efficiency[68]) based on membrane filtration where small pores allow the passage of water while blocking oils,[69] such filters have low volume throughput and can be easily clogged with excess oil (thus requiring frequent cleaning or replacement). One embodiment of the current methodology would be to deploy it for pretreatment filters installed upstream of conventional membrane filters, thereby ensuring removal of the majority of oil-based contaminants so as to minimize the

amount of oil reaching the membrane filters (therefore avoiding blockage as well as maximizing efficiency). Such oil−water separators could potentially help to tackle the environmental impact of the gas, oil, metal, textile, and food-processing industries.[70]

5. CONCLUSIONS

Solvent-cast copolymer−fluorosurfactant complexes have been found to display large-magnitude oleophobic−hydrophilic switching behavior as well as rapid switching speeds. Further enhancement in the switching performance is achieved by combining surface chemical functionality and roughness. These ultrafast switching oleophobic−hydrophilic surfaces have been shown to display excellent antifogging, self-cleaning, and oil−water separation properties.

AUTHOR INFORMATION

Corresponding Author

*E-mail: j.p.badyal@durham.ac.uk.

Notes

The authors declare no competing financial interest.

ACKNOWLEDGMENTS

We are grateful to the Engineering and Physical Sciences Research Council (Grant EP/J005401/1) and D. Carswell for DSC measurements.

REFERENCES

(1) Schaum, J.; Cohen, M.; Perry, S.; Artz, R.; Draxler, R.; Frithsen, J. B.; Heist, D.; Lorber, M.; Phillips, L. Screening Level Assessment of Risks Due to Dioxin Emissions from Burning Oil from the BP Deepwater Horizon Gulf of Mexico Spill. *Environ. Sci. Technol.* **2010**, *44*, 9383−9389.

(2) Cheng, Y.; Li, X.; Xu, Q.; Garcia-Pineda, O.; Andersen, O. B.; Pichel, W. G. SAR observation and model tracking of an oil spill event in coastal waters. *Mar. Pollut. Bull.* **2011**, *62*, 350−363.

(3) Kota, A. K.; Kwon, G.; Choi, W.; Mabry, J. M.; Tuteja, A. Hygro-responsive membranes for effective oil−water separation. *Nat. Commun.* **2012**, *3*, 1025.

(4) Kwon, G.; Kota, A. K.; Li, Y.; Sohani, A.; Mabry, J. M.; Tuteja, A. On-Demand Separation of Oil−Water Mixtures. *Adv. Mater.* **2012**, *24*, 3666−3671.

(5) Li, J.; Shi, L.; Chen, Y.; Zhang, Y.; Guo, Z.; Su, B.; Liu, W. Stable superhydrophobic coatings from thiol-ligand nanocrystals and their application in oil/water separation. *J. Mater. Chem.* **2012**, *22*, 9774−9781.

(6) Yang, H.; Lan, Y.; Zhu, W.; Li, W.; Xu, D.; Cui, J.; Shen, D.; Li, G. Polydopamine-coated nanofibrous mats as a versatile platform for producing porous functional membranes. *J. Mater. Chem.* **2012**, *22*, 16994−17001.

(7) Tian, D.; Zhang, X.; Tian, Y.; Wu, Y.; Wang, X.; Zhai, J.; Jiang, L. Photo-induced water−oil separation based on switchable super-hydrophobicity−superhydrophilicity and underwater superoleophobicity of the aligned ZnO nanorod array-coated mesh films. *J. Mater. Chem.* **2012**, *22*, 19652−19657.

(8) Brown, V. J. Industry Issues: Putting the Heat on Gas. *Environ. Health Perspect.* **2007**, *115*, A76.

(9) Adebajo, M. O.; Frost, R. J.; Kloprogge, J. T.; Carmody, R.; Kokot, S. Porous Materials for Oil Spill Cleanup: A Review of Synthesis and Absorbing Properties. *J. Porous Mater.* **2003**, *10*, 159−170.

(10) Küntzel, J.; Ham, R. Melin, Th. Regeneration of Hydrophobic Zeolites with Steam. *Chem. Eng. Technol.* **1999**, *22*, 991−994.

(11) Meininghuas, C. K. W.; Prins, R. Sorption of volatile organic compounds on hydrophobic zeolites. *Microporous Mesoporous Mater.* **2000**, *35*−*36*, 349.

(12) Alther, G. R. Organically modified clay removes oil from water. *Waste Manage.* **1995**, *15*, 623−628.

(13) Bayat, A.; Aghamiri, S. F.; Moheb, A.; Vakili-Nezhaad, G. R. Oil Spill Cleanup from Sea Water by Sorbent Materials. *Chem. Eng. Technol.* **2005**, *28*, 1525−1528.

(14) Teas, Ch.; Kalligeros, S.; Zanikos, F.; Stournas, S.; Lois, E.; Anastopoulos, G. Investigation of the effectiveness of absorbent materials in oil spills clean up. *Desalination* **2001**, *140*, 259−264.

(15) Annunciado, T. R.; Sydenstricker, T. H. D.; Amico, S. C. Experimental investigation of various vegetable fibers as sorbent materials for oil spills. *Mar. Pollut. Bull.* **2005**, *50*, 1340−1346.

(16) Sun, X.-F.; Sun, R.; Sun, J.-X. Acetylation of Rice Straw with or without Catalysts and Its Characterization as a Natural Sorbent in Oil Spill Cleanup. *J. Agric. Food Chem.* **2002**, *50*, 6428−6433.

(17) Radetić, M. M.; Jocić, D. M.; Jovančić, P. M.; Petrović, Z. L. J.; Thomas, H. F. Recycled Wool-Based Nonwoven Material as an Oil Sorbent. *Environ. Sci. Technol.* **2003**, *37*, 1008−1012.

(18) Zhu, Q.; Pan, Q.; Liu, F. Facile Removal and Collection of Oils from Water Surfaces through Superhydrophobic and Superoleophilic Sponges. *J. Phys. Chem. C* **2011**, *115*, 17464−17470.

(19) Feng, L.; Zhang, Z.; Mai, Z.; Ma, Y.; Liu, B.; Jiang, L.; Zhu, D. A Super-Hydrophobic and Super-Oleophilic Coating Mesh Film for the Separation of Oil and Water. *Angew. Chem., Int. Ed.* **2004**, *43*, 2012−2014.

(20) Wang, S.; Li, M.; Lu, Q. Filter Paper with Selective Absorption and Separation of Liquids That Differ in Surface Tension. *ACS Appl. Mater. Interfaces* **2010**, *2*, 677−683.

(21) Lee, C. H.; Johnson, N.; Drelich, J.; Yap, Y. K. The performance of superhydrophobic and superoleophilic carbon nanotube meshes in water−oil filtration. *Carbon* **2011**, *49*, 669−676.

(22) Jin, M.; Wang, J.; Yao, X.; Liao, M.; Zhao, Y.; Jiang, L. Underwater Oil Capture by a Three-Dimensional Network Architectured Organosilane Surface. *Adv. Mater.* **2011**, *23*, 2861−2864.

(23) Xue, Z.; Wang, S.; Lin, L.; Chen, L.; Liu, M.; Feng, L.; Jiang, L. A Novel Superhydrophilic and Underwater Superoleophobic Hydrogel-Coated Mesh for Oil/Water Separation. *Adv. Mater.* **2011**, *23*, 4270−4273.

(24) Howarter, J. A.; Youngblood, J. P. Amphiphile grafted membranes for the separation of oil-in-water dispersions. *J. Colloid Interface Sci.* **2009**, *329*, 127−132.

(25) Howarter, J. A.; Youngblood, J. P. Self-Cleaning and Anti-Fog Surfaces via Stimuli-Responsive Polymer Brushes. *Adv. Mater.* **2007**, *19*, 3838−3843.

(26) Howarter, J. A.; Genson, K. L.; Youngblood, J. P. Wetting Behavior of Oleophobic Polymer Coatings Synthesized from Fluorosurfactant Macromers. *ACS Appl. Mater. Interfaces* **2011**, *3*, 2022−2030.

(27) Leng, B.; Shao, Z.; de With, G.; Ming, W. Superoleophobic Cotton Textiles. *Langmuir* **2009**, *25*, 2456−2460.

(28) Wang, Y.; Dong, Q.; Wang, Y.; Wang, H.; Li, G.; Bai, R. Investigation on RAFT Polymerization of a Y-Shaped Amphiphilic Fluorinated Monomer and Anti-Fog and Oil-Repellent Properties of the Polymers. *Macromol. Rapid Commun.* **2010**, *31*, 1816−1821.

(29) Briscoe, B. J.; Galvin, K. P. The effect of surface fog on the transmittance of light. *Sol. Energy* **1991**, *46*, 191−197.

(30) Xu, F. J.; Neoh, K. G.; Kang, E. T. Bioactive surfaces and biomaterials via atom transfer radical polymerization. *Prog. Polym. Sci.* **2009**, *34*, 719−761.

(31) Kobayashi, M.; Terayama, Y.; Yamaguchi, H.; Terada, M.; Murakami, D.; Ishihara, K.; Takahara, A. Wettability and Antifouling Behavior on the Surfaces of Superhydrophilic Polymer Brushes. *Langmuir* **2012**, *28*, 7212−7222.

(32) Lampitt, R. A.; Crowther, J. M.; Badyal, J. P. S. Switching Liquid Repellent Surfaces. *J. Phys. Chem. B* **2000**, *104*, 10329−10331.

(33) Hutton, S. J.; Crowther, J. M.; Badyal, J. P. S. Complexation of Fluorosurfactants to Functionalized Solid Surfaces: Smart Behavior. *Chem. Mater.* **2000**, *12*, 2282−2286.

(34) Goddard, E. D. Polymer−surfactant interaction. Part II. Polymer and surfactant of opposite charge. *Colloids Surf.* **1986**, *19*, 301−329.

(35) Thünemann, A. F.; Lochhaas, K. H. Surface and Solid-State Properties of a Fluorinated Polyelectrolyte−Surfactant Complex. *Langmuir* **1999**, *15*, 4867−4874.
(36) Vaidya, A.; Chaudhury, M. K. Synthesis and Surface Properties of Environmentally Responsive Segmented Polyurethanes. *J. Colloid Interface Sci.* **2002**, *249*, 235−245.
(37) Li, L.; Wang, Y.; Gallaschun, C.; Risch, T.; Sun, J. Why can a nanometer-thick polymer coated surface be more wettable to water than to oil? *J. Mater. Chem.* **2012**, *22*, 16719−16722.
(38) Sawada, H.; Yoshioka, H.; Kawase, T.; Takahashi, H.; Abe, A.; Ohashi, R. Synthesis and Applications of a Variety of Fluoroalkyl End-Capped Oligomers/Silica Gel Polymer Hybrids. *J. Appl. Polym. Sci.* **2005**, *98*, 169−177.
(39) Yang, J.; Zhang, Z.; Xu, X.; Zhu, X.; Men, X.; Zhou, X. Superhydrophilic−superoleophobic coatings. *J. Mater. Chem.* **2012**, *22*, 2834−2837.
(40) Antonietti, M.; Henke, S.; Thünemann, A. F. Highly ordered materials with ultra-low surface energies: Polyelectrolyte−surfactant, complexes with fluorinated surfactants. *Adv. Mater.* **1996**, *8*, 41−45.
(41) Sawada, H.; Ikematsu, Y.; Kawase, T.; Hayakawa, Y. Synthesis and Surface Properties of Novel Fluoroalkylated Flip-Flop-Type Silane Coupling Agents. *Langmuir* **1996**, *12*, 3529−3530.
(42) Turri, S.; Valsecchi, R.; Viganò, M.; Levi, M. Hydrophilic−oleophobic behaviour in thin films from fluoromodified nanoclays and polystyrene. *Polym. Bull.* **2009**, *63*, 235−243.
(43) Bartlett, P. D.; Nozaki, K. The Polymerization of Allyl Compounds. III. The Peroxide-induced Copolymerization of Allyl Acetate with Maleic Anhydride. *J. Am. Chem. Soc.* **1946**, *68*, 1495−1504.
(44) Johnson, R. E., Jr.; Dettre, R. H. In *Wettability*; Berg, J. C., Ed.; Marcel Dekker, Inc.: New York, 1993; Chapter 1, pp 1−75.
(45) Mochizuki, C.; Hara, H.; Takano, I.; Hayakawa, T.; Sato, M. Application of carbonated apatite coating on a Ti substrate by aqueous spray method. *Mater. Sci. Eng., C* **2013**, *33*, 951−958.
(46) Kunal, K.; Robertson, C. G.; Pawlus, S.; Hahn, S. F.; Sokolov, A. P. Role of Chemical Structure in Fragility of Polymers: A Qualitative Picture. *Macromolecules* **2008**, *41*, 7232−7238.
(47) Kraus, G.; Childers, C. W.; Gruver, J. T. Properties of random and block copolymers of butadiene and styrene. I. Dynamic properties and glassy transition temperatures. *J. Appl. Polym. Sci.* **1967**, *11*, 1581−1591.
(48) López-Díaz, D.; Velázquez, M. M. Evidence of glass transition in thin films of maleic anhydride derivatives: Effect of the surfactant coadsorption. *Eur. Phys. J. E: Soft Matter Biol. Phys.* **2008**, *26*, 417−425.
(49) Kokufuta, E.; Zhang, Y.-Q.; Tanaka, T.; Mamada, A. Effects of Surfactants on the Phase Transition of Poly(*N*-isopropylacrylamide) Gel. *Macromolecules* **1993**, *26*, 1053−1059.
(50) Antonietti, M.; Conrad, J. Synthesis of Very Highly Ordered Liquid Crystalline Phases by Complex Formation of Polyacrylic Acid with Cationic Surfactants. *Angew. Chem., Int. Ed. Engl.* **1994**, *33*, 1869−1870.
(51) Ghebremeskel, A. N.; Vemavarapu, C.; Lodaya, M. Use of surfactants as plasticizers in preparing solid dispersions of poorly soluble API: Selection of polymer−surfactant combinations using solubility parameters and testing the processability. *Int. J. Pharm.* **2007**, *328*, 119−129.
(52) Grosu, G.; Andrzejewski, L.; Veilleux, G.; Ross, G. G. Relation between the size of fog droplets and their contact angles with CR39 surfaces. *J. Phys. D: Appl. Phys.* **2004**, *37*, 3350−3355.
(53) Howarter, J. A.; Youngblood, J. P. Self-Cleaning and Next Generation Anti-Fog Surfaces and Coatings. *Macromol. Rapid Commun.* **2008**, *29*, 455−466.
(54) Spatz, J. P.; Möller, M.; Noeske, M.; Behm, R. J.; Pietralla, M. Nanomosaic Surfaces by Lateral Phase Separation of a Diblock Copolymer. *Macromolecules* **1997**, *30*, 3874−3880.
(55) Su, Z.; Wu, D.; Hsu, S. L.; McCarthy, T. J. Adsorption of End-Functionalized Poly(ethylene oxide)s to the Poly(ethylene oxide)−Air Interface. *Macromolecules* **1997**, *30*, 840−845.
(56) Walters, K. B.; Schwark, D. W.; Hirt, D. E. Surface Characterization of Linear Low-Density Polyethylene Films Modified with Fluorinated Additives. *Langmuir* **2003**, *19*, 5851−5860.
(57) Qiu, G.-M.; Zhu, L.-P.; Zhu, B.-K.; Xu, Y.-Y.; Qiu, G.-L. Grafting of styrene/maleic anhydride copolymer onto PVDF membrane by supercritical carbon dioxide: Preparation, characterization and biocompatibility. *J. Supercrit. Fluids* **2008**, *45*, 374−383.
(58) Reiter, G. Dewetting as a Probe of Polymer Mobility in Thin Films. *Macromolecules* **1994**, *27*, 3046−3052.
(59) Wenzel, R. N. Resistance of Solid Surfaces to Wetting by Water. *Ind. Eng. Chem.* **1936**, *28*, 988−994.
(60) Cassie, A. B. D.; Baxter, S. Wettability of porous surfaces. *Trans. Faraday Soc.* **1944**, *40*, 546−551.
(61) Tuteja, A.; Choi, W.; Ma, M.; Mabry, J. M.; Mazzella, S. A.; Rutledge, G. C.; McKinley, G. H.; Cohen, R. E. Designing Superoleophobic Surfaces. *Science* **2007**, *318*, 1618−1622.
(62) Steele, A.; Bayer, I.; Loth, E. Inherently Superoleophobic Nanocomposite Coatings by Spray Atomization. *Nano Lett.* **2009**, *9*, 501−505.
(63) Choi, W.; Tuteja, A.; Chhatre, S.; Mabry, J. M.; Cohen, R. E.; McKinley, G. H. Fabrics with Tunable Oleophobicity. *Adv. Mater.* **2009**, *21*, 2190−2195.
(64) Tuteja, A.; Kota, A. K.; Kwon, G.; Mabry, J. M. Superhydrophilic and oleophobic porous materials and methods for making and using the same. U.S. Patent 20120000853 A1, Jan 5, 2012.
(65) Badyal, J. P. S.; Woodward, I. S. Method and apparatus for the formation of hydrophobic surfaces. World Patent 2003080258 A2, Oct 2, 2003.
(66) Gao, L.; McCarthy, T. J. The "Lotus Effect" Explained: Two Reasons Why Two Length Scales of Topography Are Important. *Langmuir* **2006**, *22*, 2966−2967.
(67) Zhao, H.; Park, K.-C.; Law, K.-Y. Effect of Surface Texturing on Superoleophobicity, Contact Angle Hysteresis, and "Robustness. *Langmuir* **2012**, *28*, 14925−14934.
(68) Compass Water Solutions. http://www.cworldwater.com (accessed July 1, 2013).
(69) Hydration Technology Innovations. http://www.htiwater.com (accessed July 1, 2013).
(70) Cheryan, M.; Rajagopalan, N. Membrane processing of oily streams. Wastewater treatment and waste reduction. *J. Membr. Sci.* **1998**, *151*, 13−28.